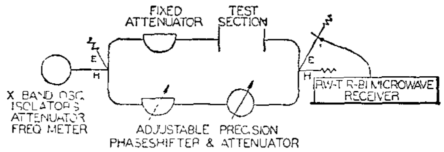

Fig. 1—The waveguide bridge circuit used to obtain the data presented in Figs. 2 and 3.

ject predicts zero degrees phaseshift across the trivial 90° branch[1,2] or clear expressions of the phaseshift are not made.[3–7]

This communication will predict the phaseshift of microwaves traveling across the collinear arms of an H-plane branch of arbitrary angle. Usually, this would be accomplished by applying complicated boundary conditions to the wave equation, however this complicated approach may not always be necessary. This communication will show a very simple method of predicting the phaseshift.

The standard waveguide bridge circuit of Fig. 1 using hybrid junctions and RG 52/U waveguide was selected as the experimental measuring device. The attenuators and phaseshifter of the bridge were precision devices. The RW-T R-B1 superheterodyne microwave receiver was used as a null detector of the bridge circuit.

A set of H-plane branches were constructed from 22.5° to 157.5° in steps of 22.5° using RG 52/U rectangular waveguide as shown in Fig. 2(a). During all tests the branch arm of the waveguide section tested was terminated with a reflectionless termination. The circles of Fig. 2(b) show the experimental results of the phaseshift across the H-plane branches from this setup. Note that the Reciprocity Theorem holds exactly; *e.g.*, the 45° branch had exactly the same phaseshift as the 135° branch.

The first attempt at explaining these experimental results was by considering the waveguide wavelength of the waves traveling across the branch to be a function of the waveguide width at that point. It is known that

$$\lambda_g(d) = \frac{\lambda_0}{\sqrt{1 + \left(\frac{\lambda_0}{2d}\right)^2}} \quad (1)$$

where d = the waveguide width where the waveguide wavelength is being considered (cm). In Fig. 2(a), ϕ = branch angle (degrees), $m = \tan\phi$, a = normal waveguide width (cm), $d = a + mz$ (cm), λ_0 = free-space wavelength (cm), z_1 = length of the branch section (cm), θ_1 = phaseshift across the H-plane branch (degrees), θ_2 = phaseshift across

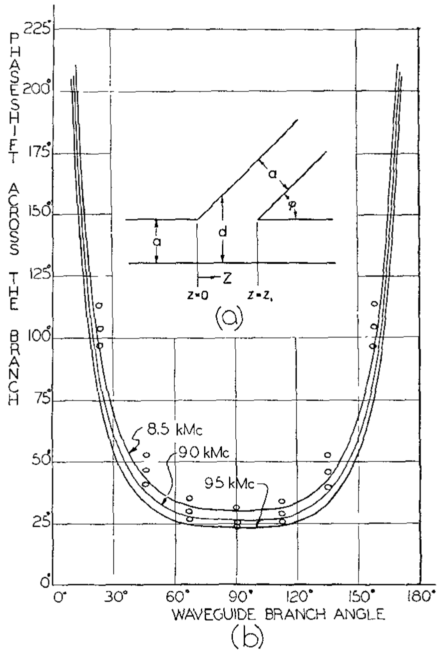

Fig. 2—(a) Waveguide H-plane junction. (b) Phaseshift across the collinear arms of H-plane waveguide branches. Circles are experimental data, curves are the theoretical phaseshifts for different frequencies; from the top, 8.5, 9.0, and 9.5 kMc.

a blank waveguide section of length z_1 (degrees), θ_T = the apparent phaseshift due to the branch in the waveguide (degrees), then

$$\theta_1 = 360 \int_0^{z_1} \frac{dz}{\lambda(d)} \quad (2)$$

$$\theta_1 = \frac{360}{m\lambda_0}\left\{\left[(a + mz_1)^2 - \frac{\lambda_0^2}{4}\right]^{1/2} - \frac{\lambda_0}{2}\cos^{-1}\left|\frac{\lambda_0}{2(a + mz_1)}\right| - \left[a^2 - \frac{\lambda_0^2}{4}\right]^{1/2} + \frac{\lambda_0}{2}\cos^{-1}\left|\frac{\lambda_0}{2a}\right|\right\} \quad (3)$$

$$\theta_2 = 360\,\frac{(z_1 - 0)}{\lambda(a)} \quad (4)$$

$$\theta_T = \theta_1 - \theta_2. \quad (5)$$

This calculation was carried out for three frequencies at all possible branch angles and found that the results broke down for angles near 90°. This was corrected by empirically keeping the waveguide width 1.170 over a distance of a, from $(z_1 - a)$ to (z_1); *e.g.*, the waveguide is considered to be $1.17a$ wide over the distance. Now we have

$$\theta_T = 360\left[\int_0^{(z_1-a)} \frac{dz}{\lambda_g(d)} - \frac{a}{\lambda(1.17a)} - \frac{(z_1 - 0)}{\lambda(a)}\right] \quad (6)$$

$$\theta_T = 360\left\{\frac{1}{m\lambda_0}\left[(a + m(z_1 - a))^2 - \frac{\lambda_0^2}{4}\right]^{1/2} - \frac{1}{2m}\cos^{-1}\left|\frac{\lambda_0}{2(a + m(z_1 - a))}\right| - \frac{1}{m\lambda_0}\left[a^2 - \frac{\lambda_0^2}{4}\right]^{1/2} + \frac{1}{2m}\cos^{-1}\left|\frac{\lambda}{2a}\right| + \frac{a}{\lambda(1.17a)} - \frac{(z_1 - 0)}{\lambda(a)}\right\}. \quad (7)$$

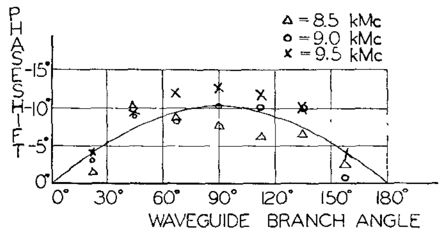

Fig. 3—Phaseshift across the collinear arms of E-plane waveguide branches. Solid curve represents the empirical equation.

This function is shown as the solid lines in Fig. 2(b) where it can be seen to predict quite satisfactorily the phaseshift across the H-plane waveguide branch.

The waveguide bridge shown in Fig. 1 was also used to measure the phaseshift across the collinear arm of a set of E-plane branches as a function of frequency and the branch angle. The experimental results are shown in Fig. 3. It was found that the phaseshift across these branches could be approximated empirically by the function,

$$\theta_T = -10.5 \sin\phi. \quad (8)$$

The solid curve in Fig. 3 represents the above empirical equation. This measured value contrasts with the phaseshift predicted for the E-plane tee by many authors.

ACKNOWLEDGMENT

The authors thank S. Krupnik, J. A. Stefancin, J. E. Billo, L. Meyer and J. Beigle for their assistance; also the Marquette University Computing Center for the use of the IBM 1620 Computer.

D. E. SCHUMACHER
K. ISHII
Dept. of Elec. Eng.
Marquette University
Milwaukee, Wis.

[1] G. C. Southworth, "Principles and Applications of Waveguide Transmission," D. Van Nostrand Co., Inc., Princeton, N. J.; 1950.
[2] H. J. Reich, P. F. Ordung, H. L. Krauss, and J. G. Skalnik, "Microwave Theory and Techniques," D. Van Nostand Co., Inc., Princeton, N. J.; 1953.
[3] H. A. Atwater, "Introduction to Microwave Theory," McGraw-Hill Book Co., Inc., New York, N. Y.; 1962.
[4] C. G. Montgomery, R. H. Dicke, and E. M. Purcell, "Principles of Microwave Circuits," McGraw-Hill Book Co., Inc., New York, N. Y.; 1948.
[5] N. Marcuvitz, "Waveguide Handbook," McGraw-Hill Book Co., Inc., New York, N. Y.; 1951.
[6] R. G. Brown, R. A. Sharpe, and W. L. Hughes, "Line, Waves and Antennas," Ronald Press Co., New York, N. Y.; 1961.
[7] T. Moreno, "Microwave Transmission Design Data," Dover Publications, New York, N. Y.; 1948.

A New High-Power Variable Attenuator*

This communication describes a design for a variable attenuator which can operate at very high peak and average power levels propagating in any chosen mode in a single or a multimode waveguide. This attenuator offers the desirable characteristics of dissipating energy in external loads rather than within the internal structure and utilizes only one coupling mechanism. The device consists of a coupled wave structure between two modes in adjacent primary and secondary waveguides, and a suitable mechanism for varying the phase constant of the secondary waveguide.

Miller[1] has shown that, when a dis-

* Received May 13, 1963. This work has been sponsored by the Wright Air Development Division under Contract No. AF33(616)6517.

[1] S. E. Miller, "Coupled wave theory and waveguide applications," *Bell Sys. Tech. J.*, vol. 33, pp. 661–719; May, 1954.

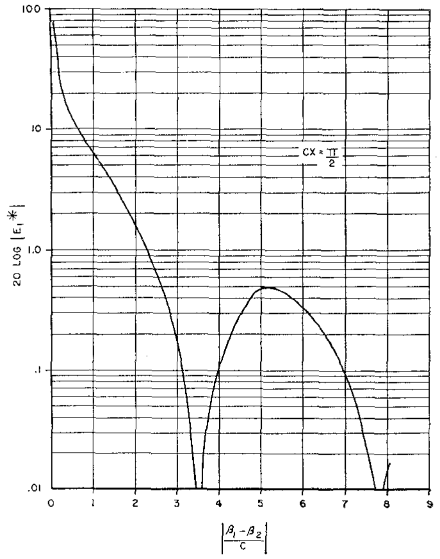

Fig. 1—The relationship of E_1^* and $\left|\frac{\beta_1-\beta_2}{C}\right|$ for $CX=\frac{\pi}{2}$.

tributed coupling region exists between lossless primary and secondary waveguides, the normalized forward traveling wave amplitude in the primary waveguide is given by

$$E_1 = \exp\left\{-jx\left(c+\frac{\beta_1+\beta_2}{2}\right)\right\}E_1^*$$

where

$$E_1^* = \cos\left[\frac{cx}{2}\sqrt{\left(\frac{\beta_1-\beta_2}{c}\right)^2+4}\right] - j\left(\frac{\beta_1-\beta_2}{c}\right)\left[\left(\frac{\beta_1-\beta_2}{c}\right)^2+4\right]^{-1/2} \cdot\sin\left[\frac{cx}{2}\sqrt{\left(\frac{\beta_1-\beta_2}{c}\right)^2+4}\right]$$

and

c = coupling strength per unit length,
x = length of coupling region,
β_1, β_2 = effective phase constants of the primary and secondary waveguides respectively.

If the coupling per unit length and the length of the coupling region are chosen such that $cx=\pi/2$, it can be shown that the magnitude of E_1 is dependent only on the quantity $(\beta_1-\beta_2)/c$. A plot of this relationship is shown in Fig. 1. From this figure it is seen that if

$$\left|\frac{\beta_1-\beta_2}{c}\right| = 0,$$

the energy entering the primary waveguide is completely transferred to the secondary waveguide; however, if

$$\left|\frac{\beta_1-\beta_2}{c}\right| \cong 3.5,$$

there is no net energy transfer between the lines. This suggests the possibility of obtain-

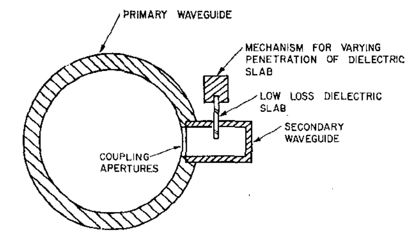

Fig. 2—Cross-sectional view of TE_{01} mode circular waveguide variable attenuator.

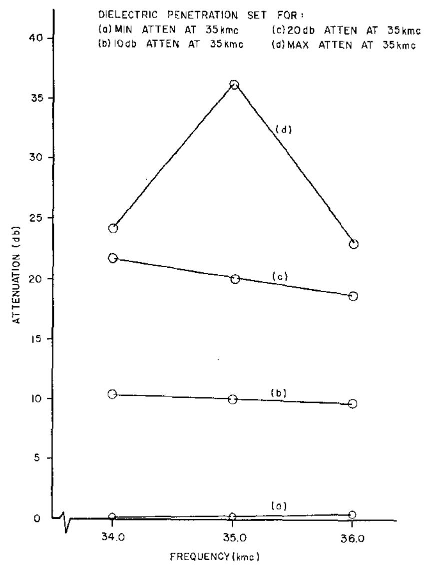

Fig. 3—Test data for TE_{01} mode circular waveguide variable attenuator.

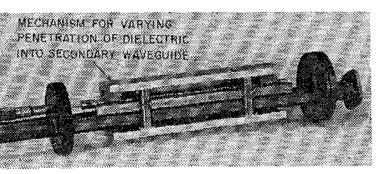

Fig. 4—TE_{01} mode circular waveguide variable attenuator.

ing a variable attenuator by terminating the secondary waveguide and making the quantity $(\beta_1-\beta_2)/c$ variable. For uniconductor waveguide structures, this can be accomplished by varying the depth of penetration of a low-loss dielectric slab into a longitudinal slot in the broad wall of the secondary waveguide.

Two experimental variable attenuators were constructed using this technique. One of these was designed to operate at 35 kMc utilizing TE_{01} mode circular waveguide as the primary waveguide and TE_{10} mode rectangular waveguide as the secondary waveguide. First the structure was designed such that complete energy transfer between the circular and rectangular waveguide would be obtained. Then, in order to make β_2 variable, a thin dielectric slab was introduced into the secondary waveguide as shown in Fig. 2. A suitable mechanism for controlling the depth of penetration of the slab also was incorporated. The data for the resultant device are given in Fig. 3, and

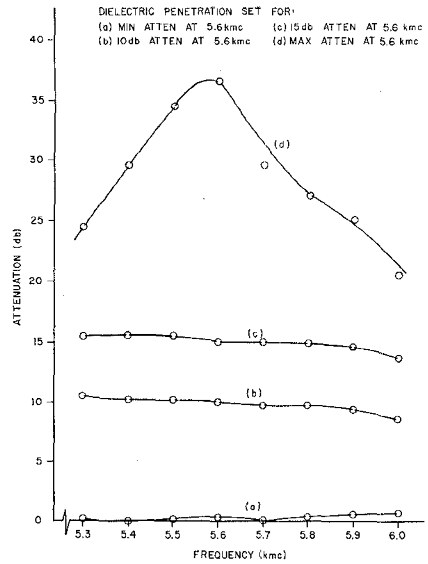

Fig. 5—Test data for rectangular waveguide variable attenuator.

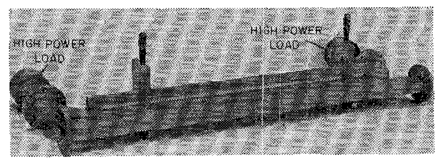

Fig. 6—Rectangular waveguide variable attenuator.

a photograph of the final device is shown in Fig. 4.

A second variable attenuator was designed to operate in the 5.4–5.9-kMc frequency range and employed dominant mode rectangular waveguide for both the primary and secondary lines. Low power data for this unit are given in Fig. 5. This unit was tested successfully at power levels up to 350 kw peak without pressurization. Fig. 6 is a photograph of the unit.

Variable attenuators of the type described in this note provide a new approach to the problem of providing power level adjustment to very high peak and average power levels. It is believed that, with careful design, attenuators can be built capable of operating at peak power levels comparable to full waveguide power with average power levels limited only by the capacity of the external loads used to terminate the secondary waveguide. Such devices can also be designed for use in multimode transmission systems such as that used to propagate the TE_{01} circular mode.

Acknowledgment

Many helpful discussions with D. C. Scott and L. K. Wilson, and the help of R. W. Coston in the experimental work presented are gratefully acknowledged.

L. R. Whicker
G. J. Neumann
Solid State and Microwave Component Development Section
Sperry Microwave Electronics Co.
Clearwater, Fla